

Right and left ventricle native T1 mapping in systolic phase in patients with congenital heart disease

Acta Radiologica
0(0) 1–7
© The Foundation Acta Radiologica
2020
Article reuse guidelines:
sagepub.com/journals-permissions
DOI: 10.1177/0284185120924563
journals.sagepub.com/home/acr



Francesco Secchi¹, Marco Ali² , Caterina B Monti² ,
Andreas Greiser³, Francesca R Pluchinotta⁴, Mario Carminati⁴
and Francesco Sardanelli^{1,2}

Abstract

Background: T1 mapping is emerging as a powerful tool in cardiac magnetic resonance (CMR) to evaluate diffuse fibrosis. However, right ventricular (RV) T1 mapping proves difficult due to the limited wall thickness in diastolic phase. Several studies focused on systolic T1 mapping, albeit only on the left ventricle (LV).

Purpose: To estimate intra- and inter-observer variability of native T1 (nT1) mapping of the RV, and its correlations with biventricular and pulmonary function in patients with congenital heart disease (CHD).

Material and Methods: In this retrospective, observational, cross-sectional study we evaluated 36 patients with CHD, having undergone CMR on a 1.5-T scanner. LV and RV functional evaluations were performed. A native modified look-locker inversion recovery short-axis sequence was acquired in the systolic phase. Intra- and inter-reader reproducibility were reported as complement to 100% of the ratio between coefficient of reproducibility and mean. Spearman ρ and Mann–Whitney *U*-test were used to compare distributions.

Results: Intra- and inter-reader reproducibility was 84% and 82%, respectively. Median nT1 was 1022 ms (interquartile range [IQR] 1108–972) for the RV and 947 ms (IQR 986–914) for the LV. Median RV–nT1 was 1016 ms (IQR 1090–1016) in patients with EDVI ≤ 100 mL/m² and 1100 ms (IQR 1113–1100) in patients with EDVI > 100 mL/m² ($P = 0.049$). A significant negative correlation was found between RV ejection fraction and RV–nT1 ($\rho = -0.284$, $P = 0.046$).

Conclusion: Systolic RV–nT1 showed a high reproducibility and a negative correlation with RV ejection fraction, potentially reflecting an adaptation of the RV myocardium to pulmonary valve/conduit (dys)-function.

Keywords

Heart ventricles, myocardium, heart defects, congenital, magnetic resonance imaging

Date received: 11 March 2019; accepted: 3 April 2020

Introduction

The use of T1 mapping in cardiac magnetic resonance (CMR) to evaluate diffuse fibrosis of the left ventricle (LV) is emerging as a powerful tool in the diagnosis of LV cardiomyopathies (1). T1 mapping provides parametric maps representing T1 values in milliseconds on a voxel-by-voxel basis. Native T1 (nT1) reflects the composition of both the intra- and extra-cellular compartment (2). Normal myocardial nT1 values at 1.5 T using modified look-locker inversion recovery (MOLLI) sequence are reported to be in the range of 895–1035 ms (3). Increased or decreased T1 values compared to this normal range were observed in several

¹Radiology Unit, IRCCS Policlinico San Donato, San Donato Milanese, Italy

²Department of Biomedical Sciences for Health, Università degli Studi di Milano, Milan, Italy

³Siemens Healthcare GmbH, Erlangen, Germany

⁴Department of Pediatric Cardiology and Adult Congenital Heart Disease, IRCCS Policlinico San Donato, San Donato Milanese, Italy

Corresponding author:

Caterina B Monti, Department of Biomedical Sciences for Health, Università degli Studi di Milano, Milan, Italy.

Email: caterina.monti@unimi.it

myocardial diseases, showing a potential of T1 mapping as a tool for clinical diagnosis (4).

In patients with congenital heart disease (CHD), CMR is a non-invasive imaging modality, highly reliable for studying heart morphology and function (5). Diagnoses and treatment planning may be based on CMR, in particular as far as the assessment of right ventricle (RV) volumes and function is concerned (6). Notably, a strong correlation can be demonstrated between late gadolinium enhancement (LGE) and histology in CHD patients (7,8). However, the role of T1 mapping in diffuse myocardial changes is still under investigation, as nT1 could be an important early indicator of cardiac dysfunction.

Kozak et al. (9) demonstrated alterations of LV and RV T1 mapping in patients with tetralogy of Fallot (ToF) using a T1 mapping sequence at the end-diastolic phase. However clinical experience suggests this approach has the limitation of such patients having a very thin RV wall, implying substantial difficulties in positioning regions of interest (ROIs) within the myocardial wall. This may also be inferred from the SDs of RV T1 times of Kozak et al. (9), which are 10 points higher than their LV counterparts. The same limitation was cited in a study published by Jellis et al. (10), that correlated RV T1 mapping with RV dysfunction in patients with non-ischemic cardiomyopathies. To overcome this limit, Kawel-Boehm et al. (11) tried to perform RV T1 mapping with a T1 mapping sequence applied at end-systolic phase. However, this sequence was only tested in healthy volunteers.

Several experiences regarding the systolic approach of T1 mapping are present in the literature (12–15). However, all these studies only focused on the LV.

The aim of the present study was to appraise intra- and inter-observer variability of nT1 mapping of the RV at systolic phase, and to analyze potential correlations between nT1 mapping of the RV and LV and functional parameters and pulmonary regurgitation in patients with CHD.

Material and Methods

Study population

The local Ethics Committee approved this study (Ethics Committee of San Raffaele University Hospital; protocol code CardioRetro; approved on 9 March 2017). This study was partially supported by Ricerca Corrente funding from Italian Ministry of Health to IRCCS Policlinico San Donato. This research received no specific grant from any funding agency in the public, commercial, or not-for-profit sectors. Due to the retrospective nature of the

present study, no specific informed consent was necessary.

We retrospectively evaluated 36 patients who underwent CMR at our institution between March 2015 and March 2017.

CMR protocol

Examinations were performed using a 1.5-T scanner (Magnetom Aera, Siemens Healthcare) with 45 mT/m gradient power, using an 18-channel surface phased-array coil placed over the thorax and with the patient in supine position.

Examinations were conducted according to standard clinical practice for patients with CHD. For each patient, LV and RV functional evaluation was performed. Every CMR study included a complete set of short-axis (from base to apex) cine images, using an electrocardiographically triggered steady-state free precession pulse sequence acquired with the following technical parameters: time of repetition (TR)/time of echo (TE) = 4.0/1.5 ms; flip angle = 80°; slice thickness = 8 mm; time resolution = 45 ms; mean acquisition time = 14 ± 4 s (mean ± SD); number of phases = 30; and in-plane pixel size = 1.40 × 1.80 mm².

Pulmonary flow analysis was performed with phase-contrast (PC) sequences and regurgitation fraction (RF) was calculated. PC through-plane sequences were used for blood flow quantification. Images perpendicular to the main pulmonary artery were acquired at about 1 cm distal from pulmonary valve. A breath-hold spoiled gradient echo sequence (fast low-angle shot) was performed for phase-velocity mapping with the following technical parameters: TR/TE = 37.12/2.47 ms; slice thickness = 5 mm; velocity encoding (VENC) = 150–350 cm/s; time resolution = 41 ms; mean acquisition time = 15 ± 4 s; and in-plane pixel size = 1.40 × 1.40 mm². Initially, we acquired the PC sequence with a VENC of 150 cm/s. In the presence of aliasing, we modified the VENC adding 50 cm/s for each new sequence.

A native MOLLI sequence with 5(3)3 protocol was acquired at the basal, ventricular level in short-axis view in systole, by starting the data acquisition at an individually adapted trigger time. The MOLLI sequence included motion correction and subsequent automatic generation of T1 maps. MOLLI sequences were acquired with the following parameters: TE/TR = 1.12/2.8 ms; flip angle = 35°; bandwidth = 1085 Hz/pixel; in-plane pixel size = 1.40 × 1.80 mm²; and parallel imaging factor = 2.

LGE sequences were acquired after intravenous administration of 0.10 mmol/kg of gadobutrol (Gadovist, Bayer Healthcare, Leverkusen, Germany) and were performed using a two-dimensional (2D)

inversion-recovery fast gradient-echo sequence. The echo time was 3.33 ms, while the repetition time was adapted to patients' heart rates, and inversion time was progressively modified from 260 ms to 330 ms, to blacken cardiac muscle; the flip angle was 25°, slice thickness was 8 mm, and pixel size was 3.6 mm².

Image assessment

A radiologist with 10 years of experience with CMR performed the segmentation of cardiac and flow images using MEDIS QMass 7.6 and QFlow 5.6 (Medis Medical Imaging Systems).

For the segmentation of cardiac images, the reader manually traced epicardial contour at both the end-diastolic and end-systolic phases. Then, a blood thresholding technique (Mass-K mode) was applied, and end-diastolic volume index with regards to body surface area (EDVI), end-systolic volume (ESVI), stroke volume (SV), and ejection fraction (EF) were calculated automatically. A 50% threshold was fixed using Mass-K mode (16).

For the segmentation of pulmonary flow, the reader selected the vessel boundary of a slice and prompted the software to propagate the segmentation through the remaining slices. The software performed an automated adjustment, and the reader could manually correct the adjusted contours. Forward flow, backward flow, and peak velocity were obtained (17).

To measure nT1 time of the RV and LV myocardium, a ROI was drawn on the end-systolic T1 maps using a freehand ROI tool. Such a ROI was drawn in each patient on the inferior wall of the basal slice to avoid blood contamination as much as possible. In order not to place the ROI in a scarred area with fibrotic tissue, LGE images were used as a reference for localization. The most appropriate imaging plane for measuring T1 time of the RV myocardium was determined by the ability to draw a ROI on the corresponding T1 map being sure not to include any adjacent blood or non-myocardial tissue only in diaphragmatic wall from short-axis views. nT1 time of the RV and LV myocardium were measured on the T1 map in the most appropriate imaging plane at end systolic phase. All measurements were performed on color-coded T1 maps as shown in Fig. 1. The window setting was individually adjusted for each T1 map, aiming not to generate homogeneously colored myocardium that could hide partial-volume effects by inclusion of adjacent blood or non-myocardial tissue. ROIs were positioned in the inferior wall of the RV, where no fibrosis was expected. To assess inter- and intra-reader reproducibility, a second reader, i.e. a radiology resident with one year of experience in CMR reperformed two additional sets of measurements of nT1 independently.

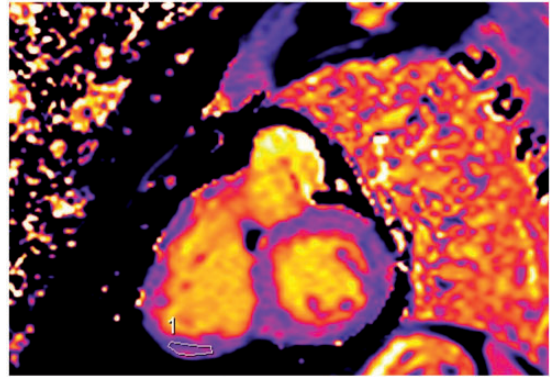


Fig. 1. Example of automatic generation of T1 maps short-axis modified look-locker inversion recovery (MOLLI) sequence at end-systolic phase. A region of interest is drawn in the basal diaphragmatic wall of the right ventricle.

Statistical analysis

Bland–Altman method was used to estimate the intra- and inter-reader reproducibility on measurements from the basal slice. The intra-reader reproducibility was performed only for the second reader, with at least a 10-day interval between the two sessions. The coefficient of repeatability (CoR) was calculated as $1.96 \times \text{SD}$ of the differences of the two datasets. Variability was reported as bias, CoR, and reproducibility (R) as complement to 100% of the ratio between CoR and bias, along with Bland–Altman plots. Correlation coefficients were classified according to Cohen (18).

Parametric variables were expressed as mean \pm SD, whereas non-parametric variables were expressed as median (interquartile ranges [IQR]). Spearman's rho was used to correlate the nT1 of RV and LV to functional parameters. The Mann–Whitney *U*-test was used to compare nT1 of RV and LV in groups of patients with different RV-EDVI. According to Maceira et al. (19), 100 mL/m² of EDVI was considered the cut-off for RV dilation.

Results

Study population and functional parameters

Our study population consisted of 36 patients (10 women; mean age = 25 ± 12 years). They represented a wide spectrum of diseases as summarized in Table 1. Functional parameters are shown in Table 2. RV nT1 was 1022 ms (IQR = 968 – 1108 ms) at the base, 962 ms (IQR = 894 – 1014 ms) at mid-level, and 956 ms (IQR = 915–1028 ms) at the apex. Moderate, positive correlations were present among nT1 values between the base and mid-level ($\rho = 0.501$, $P = 0.002$), base and apex ($\rho = 0.511$, $P = 0.001$), and a strong, positive

Table 1. Demographics, spectrum of diseases, and cardiac functional parameters.

	Patients
Patients (n)	36
Age (years)	25 ± 12
Women	10 (27)
Men	26 (73)
Congenital heart disease	
Tetralogy of Fallot	25 (69)
Aortic valve stenosis (Ross)	5 (15)
Pulmonary valve atresia	3 (8)
Pulmonary valve stenosis	3 (8)

Values are given as n (%) or mean ± SD.

Table 2. Functional parameters.

Parameters	
Left ventricle	
End-diastolic volume index (mL/m ²)	70 (63–78)
End-systolic volume index (mL/m ²)	24 (21–28)
Stroke volume (mL)	80 (66–89)
Ejection fraction (%)	64 (60–66)
Left ventricle native T1 (ms)	947 (914–986)
Right ventricle	
End-diastolic volume index (mL/m ²)	90 (72–117)
End-systolic volume index (mL/m ²)	40 (30–55)
Stroke volume (mL)	85 (69–106)
Ejection fraction (%)	54 (50–62)
Regurgitation fraction (%)	27 (8–41)
Pulmonary peak velocity (m/s)	3.2 (2.5–3.4)
Right ventricle native T1 (ms)	1022 (972–1108)

Values are given as median (interquartile range).

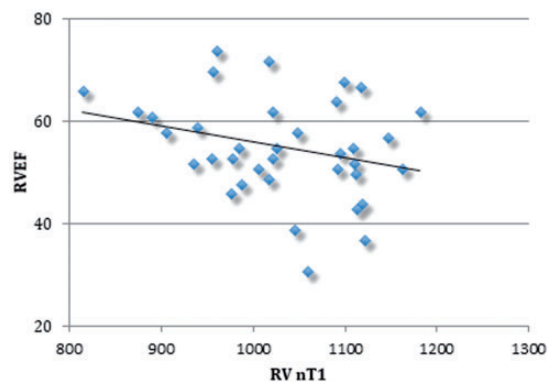
correlation was observed mid-level and apex ($\rho = 0.777$, $P < 0.001$).

Intra- and inter-reader reproducibility

Intra-reader variability analysis showed a bias of -6.81 ms and a CoR of 170 ms, thus a R of 84%, while inter-reader variability showed a bias of 3.24 ms, a CoR of 164 ms, and a R of 82%.

Correlations

A weak negative correlation was found between RVEF and RV nT1 ($\rho = -0.284$, $P = 0.046$) (Fig. 2). Regarding the LV, a moderate positive correlation was found between LVESVI and LV nT1 ($\rho = 0.396$, $P = 0.012$) (Fig. 3) and a weak borderline positive correlation was found between LVEDVI and LV nT1 ($\rho = 0.287$, $P = 0.056$). A moderate negative correlation was found between LVEF and LV nT1 ($\rho = -0.337$, $P = 0.029$) (Fig. 4). A weak borderline positive correlation was

**Fig. 2.** Correlation between RVEF and RV nT1 ($\rho = -0.284$, $P = 0.046$). RVEF, right ventricle ejection fraction; RV nT1, right ventricle native T1.

found between nT1 RV and nT1 LV ($\rho = 0.272$, $P = 0.066$). No other significant correlations were found (Table 3). Median RV nT1 was 1016 ms (IQR = 1016–1090 ms) in patients with non-pathological EDVI (≤ 100 mL/m²) and 1100 ms (IQR = 1100–1113 ms) in patients with pathological EDVI (> 100 mL/m²), with a significant difference ($P = 0.049$).

Discussion

In the present study, RV nT1 values were assessed in patients with CHD. Systolic quantification of T1 values of the RV showed a good inter- and intra-reader variability, as CoR was not too large when compared to the obtained T1 values. Another important result was the detection of a significant negative correlation between RVEF and nT1 with a good reproducibility of our measurements.

Our CHD population was characterized by normal LV function and volume, and a relative increase of RVEDVI, reflecting a dysfunction of the pulmonary valve/conduit. As is well-known, the timing of surgical/percutaneous procedure in these patients depends on clinical conditions, RV volumes, and degree of pulmonary valve dysfunction (20). However, in some cases, the remodeling of the RV is faster than expected, and the procedure is performed too late to observe a reversion of such remodeling. The possibility of measuring nT1, which reflects a fibrotic alteration of RV wall, may be used to distinguish those patients who may encounter a faster deterioration of RV volumes, and need earlier intervention.

The negative correlation between nT1 and RVEF may point that patients with an impaired RV function had an increase of mobile water species and/or interstitial deposition of collagen in the RV diaphragmatic wall. This abnormality could be correlated with RV

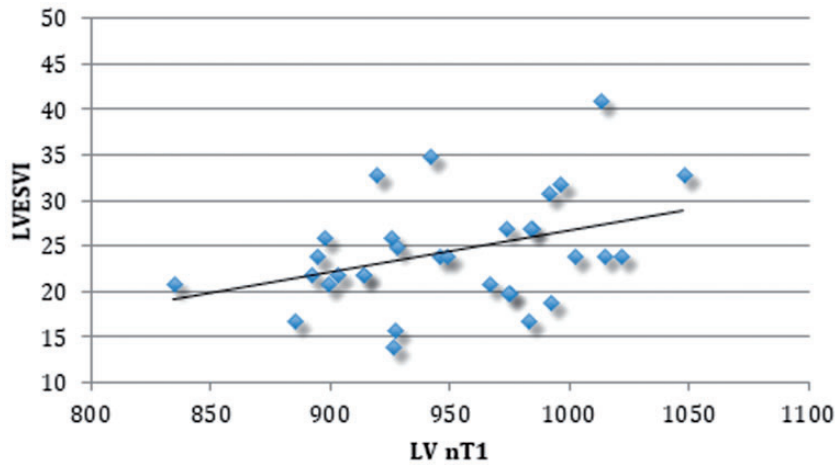


Fig. 3. Correlation between left ventricle end systolic volume (LVESVI) and left ventricle native T1 (LV nT1) ($\rho = 0.396$, $P = 0.012$).

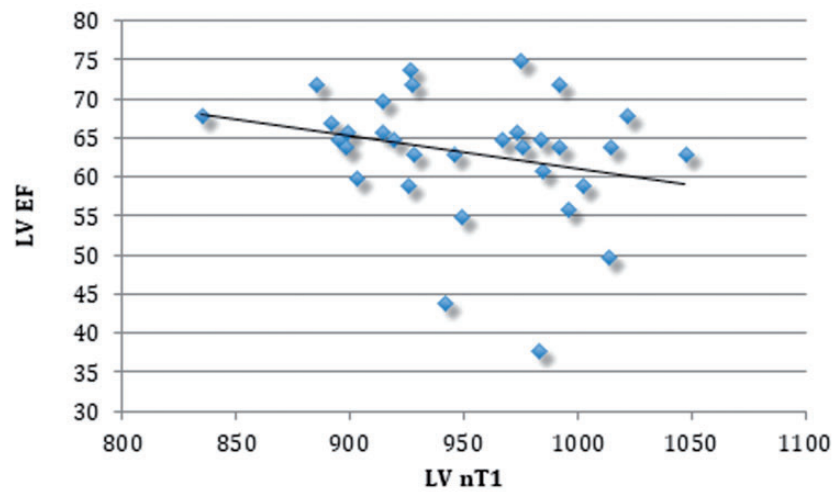


Fig. 4. Correlation between LVEF and LV nT1 ($\rho = -0.337$, $P = 0.029$). LVEF, left ventricle ejection fraction; LV nT1, left ventricle native T1.

Table 3. Correlations between functional parameters of right ventricle and left ventricle, pulmonary valve function and native T1 mapping of right and left ventricles.

	RVEDVI	RVESVI	RVS	RVEF	LVEDVI	LVESVI	LVS	LVEF	pRF	pPG	LV nT1
RV nT1	$\rho = -0.038$ $P = 0.413$	$\rho = 0.134$ $P = 0.218$	$\rho = -0.245$ $P = 0.075$	$\rho = -0.284$ $P = 0.046$	$\rho = 0.036$ $P = 0.417$	$\rho = 0.055$ $P = 0.375$	$\rho = 0.029$ $P = 0.434$	$\rho = -0.173$ $P = 0.156$	$\rho = -0.210$ $P = 0.109$	$\rho = -0.073$ $P = 0.336$	$\rho = 0.272$ $P = 0.066$
LV nT1	$\rho = 0.251$ $P = 0.830$	$\rho = 0.200$ $P = 0.136$	$\rho = 0.013$ $P = 0.471$	$\rho = -0.120$ $P = 0.257$	$\rho = 0.287$ $P = 0.056$	$\rho = 0.396$ $P = 0.012$	$\rho = -0.064$ $P = 0.364$	$\rho = -0.337$ $P = 0.029$	$\rho = -0.072$ $P = 0.348$	$\rho = 0.227$ $P = 0.106$	

The values in bold indicate statistical significance.

LVEDVI, left ventricle end-diastolic volume index; LVEF, left ventricle ejection fraction; LVESVI, left ventricle end-systolic volume index; LV nT1, native T1 mapping left ventricle; LVS, left ventricle stroke volume; pPG, pulmonary pressure gradient; pRF, pulmonary regurgitant fraction; RVEDVI, right ventricle end-diastolic volume index; RVEF, right ventricle ejection fraction; RVESVI, right ventricle end-systolic volume index; RV nT1, native T1 mapping of right ventricle; RVS, right ventricle stroke volume.

dilation and dysfunction. The existence of a positive correlation between nT1 RV and nT1 LV may be found in an increase in nT1 RV due to RV dysfunction which can be associated with a minor alteration of LV myocardium, even when LV function is preserved.

Other interesting correlations were found between LV nT1 and LV volumes as well as between LV nT1 and LVEF. An increase in LVEDVI and LVESVI and a decrease in LVEF correlated with an increase in LV nT1. These findings can be interpreted as an initial

adaptation of LV to the modifications of RV due to the LV volume overload.

Kozak et al. (9) published a similar study regarding nT1 in patients with CHD. They found an alteration of LV and RV nT1 in patients with ToF. However, in the present study a T1 mapping sequence at end-diastolic phase was used, implying substantial difficulties in positioning ROIs within a very thin RV wall. Conversely, our approach of a T1 mapping sequence acquired at end-systolic phase limited this problem.

The present study has some limitations. The first is the possibility of blood contamination of nT1 measurements in the inferior wall due to the hypertrabeculation of the RV which could potentially be supported by the fact that RV nT1 is higher than LV nT1, and the negative correlation between RVEF and RV nT1. Moreover, a larger RV volume will also mean that the wall is thinner and thus more prone to signal from blood into the RV ROI. Further studies on large, heterogeneous samples might be needed to verify whether this may stem from a systematic error due to blood contamination, or if nT1 is indeed different and thus blood contamination might be present, albeit with a non-systematic pattern. Second, we did not estimate extracellular volume fraction after intravenous administration of a gadolinium-based contrast material, while it may be an accurate biomarker for diffuse myocardial fibrosis in many cardiac diseases (21); however, contrast material injection was not included in the clinical protocol of the majority of these patients, preventing the obtaining of extracellular volume estimation. Finally, the sample size was relatively small, although measurements appear robust because a good reproducibility was obtained in spite of this limitation.

In conclusion, systolic nT1 mapping of the RV showed satisfactory reproducibility, and nT1 values obtained from mapping in systolic phase were higher in presence of lower function, potentially reflecting an adaptation of RV muscle following pulmonary valve/conduit dysfunction. This finding, however, warrants further studies on larger, heterogeneous samples for confirmation. A possible application for this new approach of end-systolic T1 mapping acquisition for RV should be the evaluation of RV nT1 in patients with pulmonary hypertension or in patients with RV failure. Due to the limits of nT1 to clearly distinguish interstitial from myocyte signal intensity, prospective studies regarding RV extracellular volume in patients with CHD are warranted.

Authors' note

Francesco Secchi is also affiliated with Department of Biomedical Sciences for Health, Università degli Studi di Milano, Milan, Italy.


Declaration of conflicting interests


The author(s) declared no potential conflicts of interest with respect to the research, authorship and/or publication of this article.

Funding

The author(s) received no financial support for the research, authorship and/or publication of this article.

ORCID iDs

Marco Ali  <https://orcid.org/0000-0001-8156-7743>

Caterina B Monti  <https://orcid.org/0000-0002-9539-8642>

References

1. Patel AR, Kramer CM. Role of cardiac magnetic resonance in the diagnosis and prognosis of nonischemic cardiomyopathy. *JACC Cardiovasc Imaging* 2017;10:1180–1193.
2. Muscogiuri G, Suranyi P, Schoepf UJ, et al. Cardiac magnetic resonance T1-mapping of the myocardium: technical background and clinical relevance. *J Thorac Imaging* 2018;33:71–80.
3. Swoboda PP, McDiarmid AK, Page SP, et al. Role of T1 mapping in inherited cardiomyopathies. *Eur Cardiol* 2016;11:96–101.
4. Chu LC, Corona-Villalobos CP, Halushka MK, et al. Structural and functional correlates of myocardial T1 mapping in 321 patients with hypertrophic cardiomyopathy. *J Comput Assist Tomogr* 2017;41:653–660.
5. Secchi F, Di Leo G, Papini GDE, et al. Cardiac magnetic resonance: impact on diagnosis and management of patients with congenital cardiovascular disease. *Clin Radiol* 2011;66:720–725.
6. Rajiah P, Tandon A, Greil GF, et al. Update on the role of cardiac magnetic resonance imaging in congenital heart disease. *Curr Treat Options Cardiovasc Med* 2017;19:2.
7. Babu-Narayan SV. Ventricular fibrosis suggested by cardiovascular magnetic resonance in adults with repaired tetralogy of Fallot and its relationship to adverse markers of clinical outcome. *Circulation* 2006;113:405–413.
8. Chowdhury UK, Sathia S, Ray R, et al. Histopathology of the right ventricular outflow tract and its relationship to clinical outcomes and arrhythmias in patients with tetralogy of Fallot. *J Thorac Cardiovasc Surg* 2006;132:270–277.
9. Kozak MF, Redington A, Yoo S-J, et al. Diffuse myocardial fibrosis following tetralogy of Fallot repair: a T1 mapping cardiac magnetic resonance study. *Pediatr Radiol* 2014;44:403–409.
10. Jellis CL, Yingchoncharoen T, Gai N, et al. Correlation between right ventricular T1 mapping and right ventricular dysfunction in non-ischemic cardiomyopathy. *Int J Cardiovasc Imaging* 2018;34:55–65.
11. Kawel-Boehm N, Dellas Buser T, Greiser A, et al. In vivo assessment of normal T1 values of the right-ventricular myocardium by cardiac MRI. *Int J Cardiovasc Imaging* 2014;30:323–328.

12. Tessa C, Diciotti S, Landini N, et al. Myocardial T1 and T2 mapping in diastolic and systolic phase. *Int J Cardiovasc Imaging* 2015;31:1001–1010.
13. Reiter U, Reiter G, Dorr K, et al. Normal diastolic and systolic myocardial T1 values at 1.5-T MR imaging: correlations and blood normalization. *Radiology* 2014;271:365–372.
14. Ferreira VM, Wijesurendra RS, Liu A, et al. Systolic ShMOLLI myocardial T1-mapping for improved robustness to partial-volume effects and applications in tachyarrhythmias. *J Cardiovasc Magn Reson* 2015;17:77.
15. Zhao L, Li S, Ma X, et al. Systolic MOLLI T1 mapping with heart-rate-dependent pulse sequence sampling scheme is feasible in patients with atrial fibrillation. *J Cardiovasc Magn Reson* 2016;18:13.
16. Secchi F, Ali M, Petrini M, et al. Blood-threshold CMR volume analysis of functional univentricular heart. *Radiol Med* 2018;123:331–337.
17. Di Leo G, D'Angelo ID, Ali M, et al. Intra- and inter-reader reproducibility of blood flow measurements on the ascending aorta and pulmonary artery using cardiac magnetic resonance. *Radiol Med* 2017;122:179–185.
18. Cohen J. *Statistical power analysis for the behavioral sciences*. London, UK: Routledge, 2013.
19. Maceira AM, Prasad SK, Khan M, et al. Reference right ventricular systolic and diastolic function normalized to age, gender and body surface area from steady-state free precession cardiovascular magnetic resonance. *Eur Heart J* 2006;27:2879–2888.
20. Secchi F, Resta EC, Cannaò PM, et al. Biventricular heart remodeling after percutaneous or surgical pulmonary valve implantation: evaluation by cardiac magnetic resonance. *J Thorac Imaging* 2017;32:358–364.
21. Cannaò PM, Altabella L, Petrini M, et al. Novel cardiac magnetic resonance biomarkers: native T1 and extracellular volume myocardial mapping. *Eur Heart J Suppl* 2016;18:E64–E71.